Nano Today (2013) **8**, 228—234

Available online at www.sciencedirect.com

SciVerse ScienceDirect

journal homepage: www.elsevier.com/locate/nanotoday

RAPID COMMUNICATION

Fabrication of metal nanoshell quantum-dot barcodes for biomolecular detection

Kun Chen, Leo Y.T. Chou, Fayi Song, Warren C.W. Chan*

Institute of Biomaterials and Biomedical Engineering, Terrence Donnelly Centre for Biomolecular Research, Materials Science and Engineering, Chemical Engineering, Chemistry, University of Toronto, 164 College Street, Toronto, Ontario M5S 3G9, Canada

Received 19 December 2012; received in revised form 25 March 2013; accepted 29 April 2013
Available online 29 May 2013

KEYWORDS
Quantum dots;
Multiplexing;
Metal nanoshell;
Biodetection;
Malaria;
Pathogen

Summary Quantum dot (QD) barcoded microbeads are a promising technology for high-throughput biodetection applications. Here we developed QD barcodes of a novel formulation to improve the bead stability, fluorescence consistency, targeting agents loading, and analytical sensitivity as well as to simplify the conjugation process. This novel formulation contains a mixed-polymer system in preparing the barcodes and a seed-mediated strategy to grow metal nanoshells on the surface of QD barcodes. The newly designed barcodes exhibited enhanced stability and a two-order improvement in analytical sensitivity compared with barcodes without any metal coating. This sensitivity enabled the barcodes to be used for multiplexed biosensing, for example, to differentiate the deadly malaria pathogen strain *Plasmodium falciparum* from the less lethal *Plasmodium vivax* specie in a single vial. Such improvements in QD barcodes properties will allow this multiplexed detection platform to emerge from academic development into broad practical applications.

Polymer microbeads are one of the most versatile platforms for chemical and biosensing applications. Microbead platforms provide faster reaction kinetics, higher throughput capacity for biomolecule conjugation, and better assay reproducibility compared to other detection techniques [1]. They could detect hundreds of molecules simultaneously when microbeads are doped with organic fluorophores or quantum dots (QDs) to create optical barcodes. Organic fluorophore-barcoded microbeads are becoming the cornerstone of multiplex detection scheme. Limitations of these barcodes include the requirement for complex and expensive read-out instruments to provide multiple light sources for exciting different fluorophores, and these barcodes can only be used in specific conditions because the emission properties of the different fluorophores are influenced differentially in biological environments. These limitations can be overcome by using QDs to create the barcodes. Over 40,000 different optical barcodes could be engineered with QDs of six different colors and intensity levels and they could be excited with light of a single wavelength [2]. Such an extensive multiplex detection technology would be extremely useful in rapid analysis of biochemical mechanisms and high-throughput screening of disease biomarkers. There are currently many proposed methods for engineering QD barcodes [2—5], but none of these methods has produced

* Corresponding author. Tel.: +1 416 946 8416; fax: +1 416 978 4317.
E-mail address: warren.chan@utoronto.ca (W.C.W. Chan).

1748-0132/$ — see front matter © 2013 Elsevier Ltd. All rights reserved.
http://dx.doi.org/10.1016/j.nantod.2013.04.009

QD barcodes with a simple conjugation process, and with good compatibility in different biological environments. Any change in the QD fluorescence during the bioassay process could lead to the misidentification of the barcodes [6,7]. Therefore, QD barcoding technology remains in the research phase and has not advanced for broader utility.

The goal of this study is to overcome the above limitations by re-formulating the barcodes and growing a metal nanoshell on QD barcode surface. First, we hypothesized that the incorporation of QDs in polymeric microbeads using a mixed-polymer system containing polystyrene and poly(styrene-co-maleic anhydride) is required to reduce the effects of pH, biological ions, and temperature on the fluorescence properties of QDs. QD fluorescence remains consistent in different biological conditions when they are at the center of sub-100-nm polystyrene beads [8]. Unfortunately, this synthetic method cannot be adapted to prepare larger beads. Conventional protocols for preparing larger beads use initiators that can quench or alter the fluorescence properties of QDs. The importance of this study from Ref. [8] is that a shell of polystyrene protects QDs from interacting with the aqueous environment. By combining polystyrene with poly(styrene-co-maleic anhydride) in the preparation of QD barcodes via a concentration-controlled flow focusing technique [3], we should expect more fluorescently stable QD barcodes.

To further improve the stability of QD barcodes and their analytical sensitivity, as well as to simplify the bioconjugation process, our strategy is to grow metal nanoshells on the surface of QD barcodes. The metal nanoshells should increase their stability by surface cross-linking the polymers, improve the analytical sensitivity by facilitating conjugation of more targeting agents and roughening the barcode surface to minimize steric interactions between the targeting agents and the target molecules, and simplify the conjugation process by eliminating the need for a coupling agent [9]. Several methods for coating bead surface with metal shells have been reported, but such metal shells are challenged with poor consistency and low ratios of surface coverage. Moreover, these metal-coated beads have not been applied in any biosensing applications [10—15].

Our overall approach for designing a metal nanoshell-coated mixed-polymer QD microbeads is illustrated in Fig. 1. First, the tri-n-octylphosphine oxide ligands on the QD surface were replaced with amino-terminated polystyrene polymers through a ligand exchange process (detailed procedure available in Supporting information). The original single-polymer system contained only poly(styrene-co-maleic anhydride) [12]. Our re-formulated mixed-polymer system contained polystyrene and poly(styrene-co-maleic anhydride). Uncoated microbeads containing QDs emitting at 555 nm (QD555) made from single polymer and mixed polymers were imaged under a wide-field microscope (Fig. 1a and b). QDs were evenly distributed in the single-polymer beads (Fig. 1a), while they were sequestered inside small droplets when a mixture of polymers was present (Fig. 1b). The maleic anhydride ring structures open up and become carboxylic acid functional groups upon contact with aqueous buffers, while the non-polar polystyrene homopolymers phase-segregate around the organic polystyrene-capped QDs.

Next, we grew a silver nanoshell on the microbead surface, which was achieved by initially modifying the surface carboxylic acid groups with cystamine via a carbodiimide-mediated reaction. The microbead surface was enriched with disulfides that strongly bind to metal nanoparticles. Microbeads were then incubated with silver nanoparticles (10 nm in diameter) as a seeding process (Fig. 1c). A silver nanoshell was grown on the surface by the addition of a reducing agent and silver nitrate. The shell thickness and surface coverage increased with prolonged growing time, and with continuous addition of reducing agent and silver nitrate. This process was characterized under a scanning electron microscope (Fig. 1c—e). The shell thickness increased to 150 nm after 2 h of growth. More detailed images are available in Supporting Fig. S2. Barcodes containing QDs of different emitting colors were coated with silver nanoshells of around 50 nm in thickness (Fig. 1f—h). The fluorescence of QD barcodes remained distinct under a wide field microscope. It suggests that a metal nanoshell with controlled thickness would not critically affect the barcoding capacity of QDs. The fluorescence intensities of QD microbeads decreased with increased shell thickness (Fig. 1i) since less photons could penetrate into and through the microbeads with a thicker shell. The decrease in fluorescence with respect to increase in silver nanoshell thickness was similar for single- and mixed-polymer barcodes, and also for barcodes containing different emitting QDs (Supporting Figs. S3 and S4). Silver nanoshells only decreased the fluorescence intensity of QD barcodes, but did not shift their emitting wavelength (Supporting Fig. S5). Therefore, in practical applications the thickness of the nanoshells should be controlled to allow the fluorescence to be excited and captured by the camera or photodetectors for proper identification of the barcodes. Interestingly, different shell thicknesses could also be used to increase the number of QD barcodes since the thickness would influence the fluorescence intensities. Future studies should focus on characterizing the long-term stability of the silver nanoshells to ensure the shell thickness is intact in storage since silver nanoparticles are prone to oxidation. Aside from silver, we can also grow gold nanoshells on the surface (Supporting Figs. S6 and S7). However, in this study we chose to optimize the silver shells versus gold shells for the biodetection assays because gold nanoshells have a maximum plasmon peak at 520 nm. Many secondary probes used in assays emit in the visible wavelength range, and therefore, the gold nanoparticles may quench the probe's fluorescence. The fact that silver nanoparticles absorb around 420 nm would provide greater selection of secondary dye molecules.

Once we have prepared these metal nanoshell-coated barcodes, we next evaluated the fluorescence stabilities and their shelf-life (which refers to the ability of beads to remain intact in biological buffers). For this study, we compared uncoated single-polymer, and silver nanoshell-coated single- and mixed-polymer barcodes. We did not include the uncoated mixed-polymer barcodes because we found that the polymer composition did not significantly affect their shelf-life (Supporting Fig. S8). Barcodes with different designs were treated with different conditions: pHs from 4 to 11 (Fig. 2a—c), buffers including water, HEPES (no sodium chloride), TE (no sodium chloride), PBS (137 mM

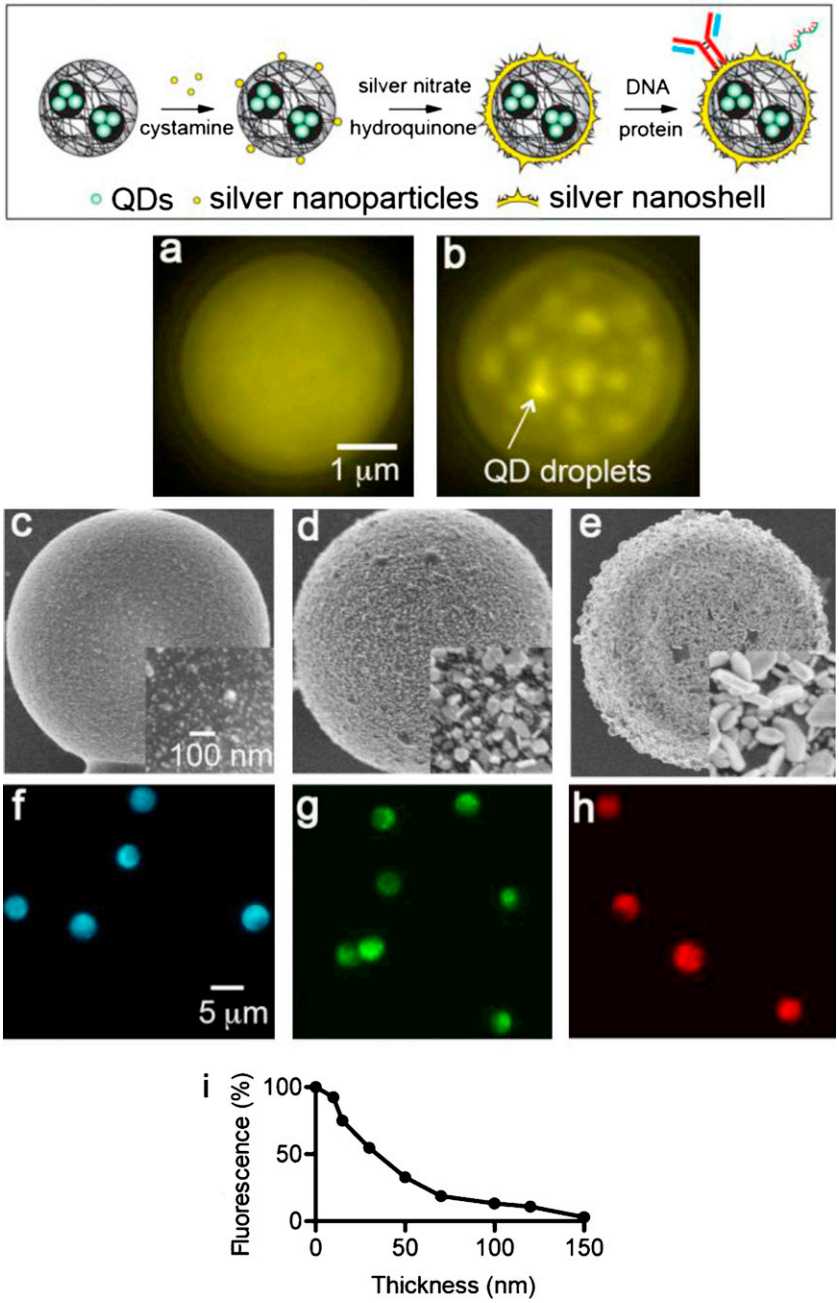

Figure 1 Morphology and fluorescence of silver nanoshell-coated QD microbeads. The process of fabricating and functionalizing silver nanoshell-coated QD microbeads is illustrated in the top scheme. (a and b) Fluorescence images of uncoated microbeads containing QD555 (λ_{em} = 555 nm) made from (a) poly(styrene-co-maleic anhydride) single polymer or (b) poly(styrene-co-maleic anhydride)—polystyrene mixed polymers. (c—e) Scanning electron microscopy images (obtained at 2 kV) of microbeads with a silver nanoshell growing for different durations. (c) Beads seeded with 10-nm silver nanoparticles, (d) grew for 30 min, average d = 70 nm, (e) grew for 120 min, average d = 150 nm. (a—e) Scale: single image size is 4 μm × 4 μm, and inset image size is 500 nm × 500 nm. (f—h) Fluorescence images of silver nanoshell-coated microbeads containing (f) QD510, (g) QD575 and (h) QD665. The thickness of the silver nanoshells was all approximately 50 nm. Single image size is 40 μm × 40 μm. All the fluorescence images were acquired through a long-pass (>430 nm) filter with a mercury lamp excitation (λ_{ex} = 350/50) and 100× UPlanApo objective (NA = 1.35). (i) Correlation of the fluorescence intensity of beads with the thickness of the silver nanoshell. The fluorescence intensity of uncoated beads was converted to 100% and other groups were normalized accordingly.

of sodium chloride) and SSC (150 mM of sodium chloride) (Fig. 2d—f), and temperatures from 25 to 90 °C (Fig. 2g—i). We used flow cytometry to characterize the fluorescence intensity of the beads instead of using a fluorometer, as described in our previous study [3]. We now recognize that a fluorometer cannot distinguish intact and degraded QD barcodes. The fluorescence intensities are expressed relative to the control conditions of each group, i.e. pH 7, water,

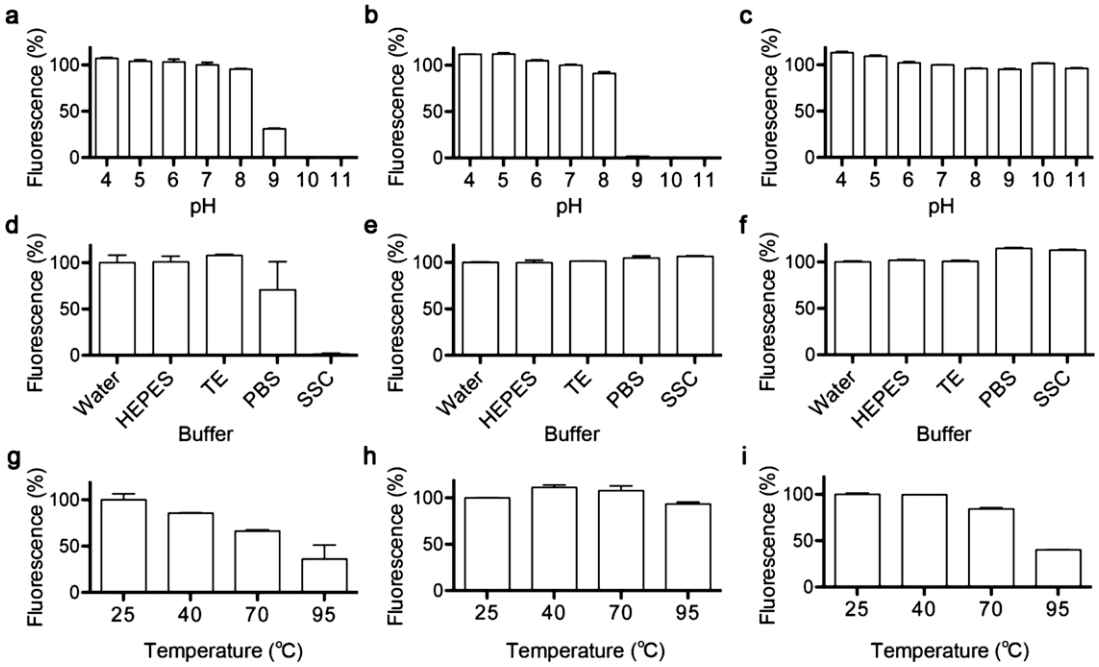

Figure 2 Fluorescence stabilities of QD microbeads made from different compositions under environmental conditions. Microbeads made from three compositions were prepared. Left column (a, d, g): uncoated poly(styrene-co-maleic anhydride) single polymer; middle column (b, e, h): silver nanoshell-coated single polymer; right column (c, f, i): silver nanoshell-coated poly(styrene-co-maleic anhydride)—polystyrene mixed polymers. The silver nanoshells were 20—30 nm in thickness. Microbeads were incubated in pH 4—11 for 24 h (a—c), or in water, HEPES (pH 7), TE (pH 8), PBS (pH 7) and SSC (pH 7) buffer for 24 h (d—f), or in 25—95 °C for 20 min (g—i). The median fluorescence intensities of microbeads were determined by flow cytometry after treatment. In each condition, the intensity values of microbeads at pH 7, water and 25 °C were converted to 100% and other groups were normalized accordingly.

and temperature at 25 °C. The fluorescence of uncoated single-polymer beads dropped dramatically at pHs above 8, buffers with a salt concentration of over 100 mM, and temperatures over 40 °C (Fig. 2a, d, g). Compared to uncoated beads, a silver nanoshell significantly improved the fluorescence stability of both the single- and mixed-polymer microbeads under tested buffer and temperature conditions. We also used flow cytometer to evaluate the shelf-life. The forward scattering and side scattering plots suggest that uncoated beads degraded easily under alkaline, high ionic strength, and high heat conditions (Supporting Fig. S9). With a silver nanoshell, microbeads remained intact under these conditions. The bead structure was maintained by the hydrophobic interactions among the polymer chains for the uncoated barcodes and these non-covalent stabilizing interactions can be disrupted by ions and temperature that cause them to break. The silver nanoshell functioned as a surface crosslinker and protected the beads from breaking. However, silver nanoshell-coated single-polymer beads were intact but their fluorescence was changed by high pHs (Fig. 2b). The reason may be that the silver nanoshell did not completely cover the surface and hydroxyl ions were able to penetrate into beads and interact with QDs inside. Beads made of mixed polymers with silver nanoshells demonstrated the best compatibility with pH from 4 to 11, all buffers, and temperatures up to 70 °C (Fig. 2c, f, i). The unique phase-segregated domains within the microbeads prevented aqueous ions from contacting and interacting with the QDs. Therefore, the silver nanoshells and mixed polymers are both critical to achieve the best fluorescence stability and structure integrity of the QD barcodes. Gold nanoshells exhibited a similar protective effect on barcode fluorescence (Supporting Fig. S10).

We then compared the analytical performance of uncoated and silver nanoshell-coated microbeads in biodetection assays. The positive control DNA strand used in the multiplexed experiments was chosen as the model target. Uncoated QD555 beads were conjugated with aminated capture probes of target strand by a carbodiimide coupling agent. The conjugation conditions were optimized in previous studies [16,17]. Silver nanoshell-coated beads were functionalized with thiolated capture probes. The amount of capture probes for conjugation was kept the same for the uncoated and silver nanoshell-coated QD barcodes. The target strands were then measured by a sandwich assay performed in parallel using both types of beads. The limit of detection was determined by 3 standard deviations above the negative control. The silver nanoshell-coated beads demonstrated a much better fitting curve (R^2 value) than the uncoated beads at the low concentration range of target strands. These values are available in Supporting Table S1. Uncoated beads had a detection limit of 0.4 fmol. This sensitivity is consistent with our previous studies [16,17]. Silver nanoshell-coated beads exhibited a detection limit of 3 amol, which was a 2-order improvement over uncoated beads (Fig. 3). With these experiments, we purposely selected SSC buffers for comparison despite Fig. 2 showing the uncoated single polymer microbeads led to

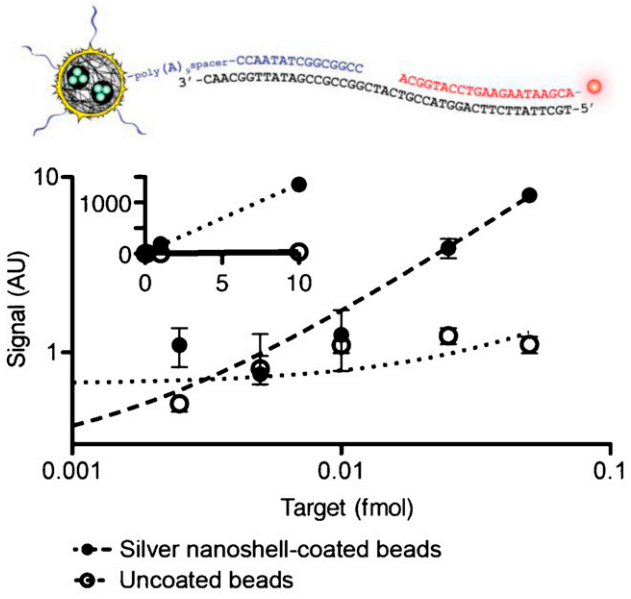

Figure 3 Comparison of assay sensitivities using uncoated and silver nanoshell-coated microbeads. The sandwich assay is illustrated in the top scheme. Uncoated microbeads were conjugated with aminated capture probes by carbodiimide chemistry, and silver nanoshell-coated microbeads (about 50 nm in thickness) were functionalized with thiolated capture probes. The sequences of the capture probes contained a 9-adenosine (A) spacer region at the 5′-end. The assays were carried out in parallel using both types of microbeads. Up to 10 fmol of target were measured (inset figure). Black solid dots and hollow circles represent the silver nanoshell-coated beads and uncoated beads, respectively.

degradation of uncoated single polymer beads. The main reason is that SSC is the most commonly used buffered system for DNA hybridization and that the manipulation of the sodium chloride concentration can lead to better DNA hybridization efficiency. To ensure that the comparison is fair, we reduced the salt concentration by 4 times and the experiments were done in 20 min to minimize the rate of degradation. For Fig. 2, the beads were exposed for 24 h. We confirmed the uncoated single polymer beads were intact by using flow cytometry at reduced SSC salt concentration and at 20 min (Supporting Fig. S11). Similar experimental conditions were used in our previous study [16]. This result now suggests the stability of the nanoshell-coated microbeads will allow us to further increase salt concentration to improve hybridization efficiency in future experiments. The detection sensitivity by silver nanoshell-coated beads was achieved by a 1-step 20-min sandwich assay without any signal amplification process. These findings are the first results demonstrating that a metal nanoshell on microbead surface significantly improves the biodetection sensitivity. There were several potential mechanisms contributing to the signal enhancement. First, the silver nanoshells increased the total surface area of barcodes and there were about 3 times more capture probes on each silver-nanoshell coated bead than the uncoated bead (Supporting Table S2). As a result, the target strands would have a higher chance to be captured by the silver nanoshell-coated barcodes. The increased amount of capture probes on the bead surface is obviously not sufficient to account for the whole increase in detection sensitivity. Another mechanism may be that silver nanoshells significantly roughened bead surface and reduced the steric hindrance by the capture probes. For uncoated beads, we found the steric effects of capture probes would significantly decrease the analytical sensitivity [16]. The capture probes on a roughened surface would be more disordered, which minimizes the steric interactions between target molecules and capture probes. The uncoated beads also showed a higher level of non-specific binding of reporter probes compared to the silver nanoshell-coated beads, leading to a higher background signal and reduced detection sensitivity (Fig. 3). We also suspected that the silver nanoshells may exert metal enhanced fluorescence effect on the reporter fluorophores. Silver nanoparticles can enhance the fluorescence intensity of fluorophores in a distance- and thickness-dependent manner [18,19]. For Alexa647 used in these assays, strong metal enhanced fluorescence can occur at a distance of 15—50 nm away from the silver nanoparticles of a thickness/diameter of 10—150 nm [20,21]. In the present design, the distance between Alexa647 and the silver nanoshell was about 25 nm based on the lengths of the capture probe and reporter probe (sequences available in Supporting information), within the range for metal enhanced fluorescence. It is more probable that the combination of the above and other unknown factors led to the final enhancement of biodetection sensitivity. More studies are needed to elucidate which mechanism contributes more than others, and the results would be useful to further improve assay sensitivity.

Finally, we demonstrated the practical application of the silver nanoshell-coated QD barcodes in multiplexed biodetection by conducting a 4-plex DNA assay for differentiation of *Plasmodium falciparum*, a deadly specie of malaria, from other nonlethal malaria species. Over 1 million people die from malaria infections annually [22,23]. There are four different parasites that cause malaria in humans: *P. falciparum*, *Plasmodium vivax*, *Plasmodium ovale*, and *Plasmodium malariae*. The ability to differentially identify the deadly *P. falciparum* from the other species is important for proper clinical treatment of patients and to reduce drug resistance. However, drug resistance to antimalarial drugs is rampant because the improper drug administration for treatment of the wrong malarial species exacerbates drug resistance. In order to detect *P. falciparum* from other malarial species, we first designed capture probes based on genetically conserved regions of the 18S rRNA gene of *P. falciparum* and *P. vivax* [24,25], and an Alexa647-labeled reporter probe. Negative and positive control strands were also designed (sequences available in Supporting information). Silver nanoshell-coated QD barcodes of four different fluorescent signatures were functionalized with thiolated capture probes for each target [26]. The dose—response curves of *P. falciparum* and *P. vivax* are shown in Fig. 4a and b. Both target strands showed excellent linearity between their concentrations and the assay signals. The signal intensity of *P. vivax* was about one order higher than that of *P. falciparum*. We observed similar phenomena in our other studies [16]. Different DNA targets exhibit different assay signal intensities, caused by their differences in secondary structures of capture probes and target strands, melting

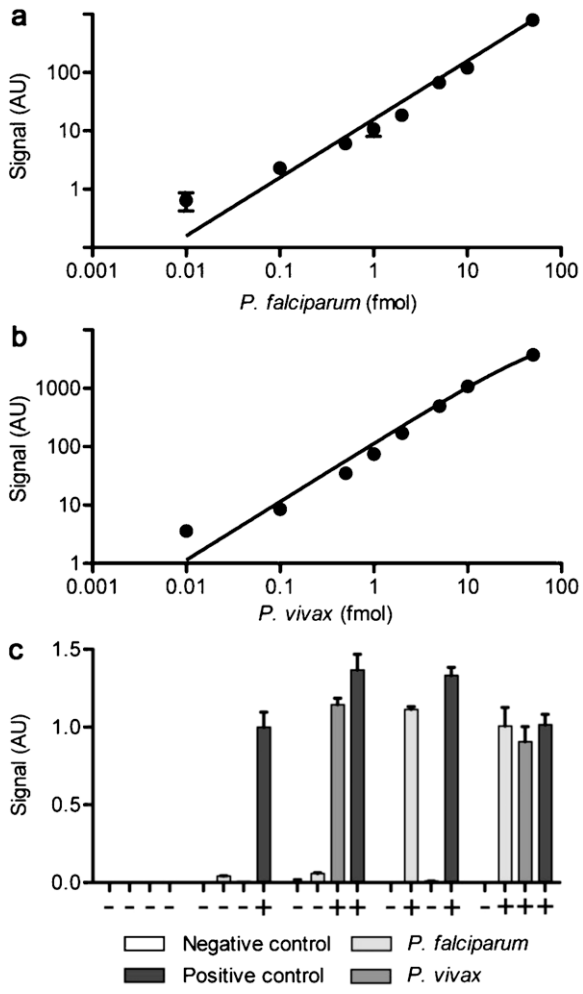

Figure 4 Multiplexed detection of DNA targets by silver nanoshell-coated QD barcodes. Silver nanoshell (about 50 nm in thickness)-coated beads were functionalized with thiolated capture probes for four strands, including a negative control strand, a positive control strand, *P. falciparum* target strand and *P. vivax* target strand. (a and b) The dose—response curves of *P. falciparum* and *P. vivax*, respectively. Up to 10 fmol of target strands were measured by the assay. The error bars in the dose—response curve of *P. vivax* (b) are small and included. (c) Multiplexed detection of DNA targets. Five mock DNA samples were tested: all negative, the positive control only, *P. vivax* plus the positive control, *P. falciparum* plus the positive control, and *P. vivax*, *P. falciparum* plus the positive control. The target strands were all 10 fmol in the experiments if they were present in the samples. Signal values of each strand in the multiplexed assays were normalized by the signal value of its pure strand (10 fmol).

temperatures, and conjugation efficiencies. To investigate the cross-reactivity among target strands, five different mock genetic samples were prepared by mixing different combinations of the target strands plus a positive control strand (10 fmol). There was negligible nonspecific binding of the reporter probe to silver nanoshell-coated beads as shown in the all-negative group. The target strands did not affect each other's signal, suggesting no cross-reactivity between the targets (Fig. 4c). Our results clearly demonstrate the ability of these barcodes to differentiate different strains of malaria parasites in a single reaction vial. The current gold standard method for differentiating malaria species is lateral flow assays using protein biomarkers [27]. This clinically approved technique can only detect *P. falciparum* and the other malarial species at high parasitemia (i.e. parasite burden in the blood) but are much less reliable in infections with low parasitemia [28]. PCR diagnostic techniques have much better analytical sensitivity than lateral flow assays and can differentiate malarial species but PCR will be difficult for use in the field or remote settings. Our current analytical sensitivity is close to that of PCR but bead assays can be easily automated and detected using microscopy, fluorometer, and flow cytometry. Hence, the bead assays would provide much greater probability of being used in the field in comparison to PCR.

In conclusion, we have developed a method to synthesize metal nanoshell-coated QD barcodes. The diameter of microbeads, the fluorescence of QDs, and the thickness of metal nanoshell are highly tunable. The fluorescence of these QD barcodes has greater consistency in a wide range of pH, buffer and temperature conditions. This should lead to improvements in the identification of the barcodes. We also observed a 2-order increase in analytical sensitivity for detecting genetic targets using metal nanoshell-coated microbeads in comparison to uncoated microbeads. The assay process is very simple, reliable and fast, and the detection sensitivity is comparable to other bead-based detection platforms with signal amplification mechanisms [29,30]. Finally, these composite microbeads are capable of multiplexed biodetection with excellent barcoding performance. We show that the barcodes can identify the deadly malaria pathogen strain from other species. These advantages make this platform an ideal candidate for ultrasensitive and high-throughput multiplexed biosensing applications in biology research and clinical diagnosis.

Author contributions

The manuscript was written through contributions of all authors. All authors have given approval to the final version of the manuscript.

Funding sources

This work was supported by Canadian Health Research Program, Canadian Foundation for Innovation, Natural Sciences and Engineering Research Council (NSERC), Canadian Institute of Health Research, Canada Research Chairs Program.

Acknowledgments

We would like to acknowledge Drs. Anu Rebbapragada, Vanessa Allen, Yali Gao, and Mr. Stephen Perusini for technical discussion. We also thank Dr. Peter Zandstra for use of the flow cytometer. Mr. Leo Chou would like to acknowledge the Teresina Florio Graduate Scholarship, the Frank Fletcher Memorial Award, the Paul and Sally Wang Graduate Scholarship, and NSERC for financial support.

Appendix A. Supplementary data

Supplementary data associated with this article can be found, in the online version, at http://dx.doi.org/10.1016/j.nantod.2013.04.009.

References

[1] R. Wilson, A.R. Cossins, D.G. Spiller, Angew. Chem. Int. Ed. Engl. 45 (2006) 6104—6117.
[2] M. Han, X. Gao, J.Z. Su, S. Nie, Nat. Biotechnol. 19 (2001) 631—635.
[3] S. Fournier-Bidoz, T.L. Jennings, J.M. Klostranec, W. Fung, A. Rhee, D. Li, W.C. Chan, Angew. Chem. Int. Ed. Engl. 47 (2008) 5577—5581.
[4] X. Gao, S. Nie, J. Phys. Chem. B 107 (2003) 11575—11578.
[5] D. Wang, A.L. Rogach, F. Caruso, Nano Lett. 2 (2002) 857—861.
[6] X. Gao, W.C. Chan, S. Nie, J. Biomed. Opt. 7 (2002) 532—537.
[7] J.A. Lee, A. Hung, S. Mardyani, A. Rhee, J. Klostranec, Y. Mu, D. Li, W.C. Chan, Adv. Mater. 19 (2007) 3113—3118.
[8] L.Y. Chou, W.C. Chan, Nanomedicine (London) 6 (2011) 767—775.
[9] M. Brust, D.J. Schiffrin, D. Bethell, C.J. Kiely, Adv. Mater. 7 (1995) 795—797.
[10] Y.C. Cao, X.F. Hua, X.X. Zhu, Z. Wang, Z.L. Huang, Y.D. Zhao, H. Chen, M.X. Liu, J. Immunol. Methods 317 (2006) 163—170.
[11] T. Ji, V.G. Lirtsman, Y. Avny, D. Davidov, Adv. Mater. 13 (2001) 1253—1256.
[12] J.H. Lee, M.A. Mahmoud, V. Sitterle, J. Sitterle, J.C. Meredith, J. Am. Chem. Soc. 131 (2009) 5048—5049.
[13] K.E. Peceros, X. Xu, S.R. Bulcock, M.B. Cortie, J. Phys. Chem. B 109 (2005) 21516—21520.
[14] A.D. Quach, G. Crivat, M.A. Tarr, Z. Rosenzweig, J. Am. Chem. Soc. 133 (2011) 2028—2030.
[15] W. Shi, Y. Sahoo, M.T. Swihart, P.N. Prasad, Langmuir 21 (2005) 1610—1617.
[16] Y. Gao, W.L. Stanford, W.C. Chan, Small 7 (2011) 137—146.
[17] S. Giri, E.A. Sykes, T.L. Jennings, W.C. Chan, ACS Nano 5 (2011) 1580—1587.
[18] A.I. Dragan, E.S. Bishop, J.R. Casas-Finet, R.J. Strouse, M.A. Schenerman, C.D. Geddes, Anal. Biochem. 396 (2010) 8—12.
[19] C.R. Sabanayagam, J.R. Lakowicz, Nucleic Acids Res. 35 (2007) e13.
[20] E.G. Matveeva, I. Gryczynski, A. Barnett, Z. Leonenko, J.R. Lakowicz, Z. Gryczynski, Anal. Biochem. 363 (2007) 239—245.
[21] J. Zhang, E. Matveeva, I. Gryczynski, Z. Leonenko, J.R. Lakowicz, J. Phys. Chem. B 109 (2005) 7969—7975.
[22] Y. Kockaerts, S. Vanhees, D.C. Knockaert, J. Verhaegen, M. Lontie, W.E. Peetermans, Eur. J. Emerg. Med. 8 (2001) 287.
[23] P. Martens, L. Hall, Emerg. Infect. Dis. 6 (2000) 103.
[24] M. Ndao, E. Bandyayera, E. Kokoskin, T.W. Gyorkos, J.D. MacLean, B.J. Ward, J. Clin. Microbiol. 42 (2004) 2694—2700.
[25] G. Snounou, S. Viriyakosol, X.P. Zhu, W. Jarra, L. Pinheiro, V.E. do Rosario, S. Thaithong, K.N. Brown, Mol. Biochem. Parasitol. 61 (1993) 315.
[26] H.D. Hill, J.E. Millstone, M.J. Banholzer, C.A. Mirkin, ACS Nano 3 (2009) 418—424.
[27] M.L. Wilson, Clin. Infect. Dis. 54 (2012) 1637—1641.
[28] M.L. McMorrow, M. Aidoo, S.P. Kachur, Clin. Microbiol. Infect. 17 (2011) 1624—1631.
[29] S.C. Chapin, P.S. Doyle, Anal. Chem. 83 (2011) 7179—7185.
[30] E. Schopf, Y. Chen, Anal. Biochem. 397 (2010) 115—117.

Kun Chen received his PhD from the University of Saskatchewan, Canada in 2009. At present he is working as a postdoctoral fellow in Dr. Warren Chan's Laboratory in the Institute of Biomaterials and Biomedical Engineering, University of Toronto. His research areas include development of novel biosensing platforms using nanomaterials for biology research and clinical diagnosis.

Leo Chou is currently pursuing his PhD with Dr. Warren Chan in the Institute of Biomaterials and Biomedical Engineering at the University of Toronto. He received his BASc in Biomedical Engineering from the University of Toronto prior to joining Dr. Chan's group. His current research focuses on nanoparticle design for delivery applications.

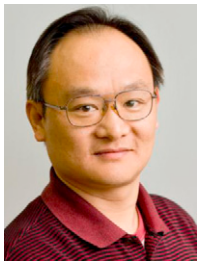

Fayi Song received his MSc (1991) from the Changchun Institute of Applied Chemistry, Chinese Academy of Sciences, and PhD (2000) from Hong Kong. He has since worked at California State University-Los Angeles, Clemson University, and the University of Toronto for his postdoctoral research. In 2008, he joined Prof. Warren Chan's group as Research Associate and recently Lab Manager. His current research interests focus on preparation, functionalization, and application of nanoparticles as well as multifunctional nanostructures.

Warren C.W. Chan received his BS from the University of Illinois in Champaign-Urbana, PhD from Indiana University, and postdoctoral training at the University of California-San Diego. He is currently a full professor at the University of Toronto and currently the Canadian Research Chair in Nanomedicine. His research interest is in the development of nanotechnology for cancer and infectious disease applications.